Breast DWI at 3 T: influence of the fat-suppression technique on image quality and diagnostic performance

Luisa Nogueira [a,b,*], Sofia Brandão [c], Rita G. Nunes [d], Hugo Alexandre Ferreira [d], Joana Loureiro [c], Isabel Ramos [b]

[a] *Department of Radiology, School of Health Technology of Porto/Polytechnic Institute of Porto (ESTSP/IPP), Rua Valente Perfeito, 4400-330, Vila Nova de Gaia, Portugal*
[b] *Department of Radiology, Hospital de São João/Faculty of Medicine of Porto University (FMUP), Alameda Prof. Hernani Monteiro, 4200-319 Porto, Portugal*
[c] *MRI Unit, Department of Radiology, Hospital de São João, Alameda Prof. Hernani Monteiro, 4200-319 Porto, Portugal*
[d] *Institute of Biophysics and Biomedical Engineering (IBEB), Faculty of Sciences, University of Lisbon, Campo Grande, 1749-016, Lisboa, Portugal*

AIM: To evaluate two fat-suppression techniques: short tau inversion recovery (STIR) and spectral adiabatic inversion recovery (SPAIR) regarding image quality and diagnostic performance in diffusion-weighted imaging (DWI) of breast lesions at 3 T.

MATERIALS AND METHODS: Ninety-two women (mean age 48 ± 12.1 years; range 21−78 years) underwent breast MRI. Two DWI pulse sequences, with b-values (50 and 1000 s/mm^2) were performed with STIR and SPAIR. The signal-to-noise ratio (SNR), contrast-to-noise ratio (CNR), suppression homogeneity, and apparent diffusion coefficient (ADC) values were quantitatively assessed for each technique. Values were compared between techniques and lesion type. Receiver operating characteristics (ROC) analysis was used to evaluate lesion discrimination.

RESULTS: One hundred and fourteen lesions were analysed (40 benign and 74 malignant). SNR and CNR were significantly higher for DWI-SPAIR; fat-suppression uniformity was better for DWI-STIR ($p < 1 \times 10^{-4}$). ADC values for benign and malignant lesions and normal tissue were 1.92×10^{-3}, 1.18×10^{-3}, 1.86×10^{-3} s/mm^2 for DWI-STIR and 1.80×10^{-3}, 1.11×10^{-3}, 1.79×10^{-3} s/mm^2 for SPAIR, respectively. Comparison between fat-suppression techniques showed significant differences in mean ADC values for benign ($p = 0.013$) and malignant le-sions ($p = 0.001$). DWI-STIR and -SPAIR ADC cut-offs were 1.42×10^{-3} and 1.46×10^{-3} s/mm^2, respectively. Diagnostic performance for DWI-STIR versus SPAIR was: accuracy (81.6 versus 83.3%), area under curve (87.7 versus 89.2%), sensitivity (79.7 versus 85.1%), and specificity (85 versus 80%). Positive predictive value was similar.

CONCLUSION: The fat-saturation technique used in the present study may influence image quality and ADC quantification. Nevertheless, STIR and SPAIR techniques showed similar diagnostic performances, and therefore, both are suitable for use in clinical practice.

Introduction

The role of diffusion-weighted MRI (DWI) in the characterization and differentiation of breast lesions remains a subject of intensive research.[1–3] In breast DWI, the use of an effective fat-suppression technique is especially critical. As the MRI signal has contributions from both water and fat components,[4] it is essential to efficiently eliminate the lipid signal. The fat fraction in breast tissue can be high, and as the apparent diffusion coefficient (ADC) of fat is much lower than that of water within lesions and/or normal glandular tissue,[5] the presence of lipids may compromise an accurate ADC estimate.

Multiple fat-suppression techniques are currently available [short tau inversion recovery (STIR), spectral adiabatic inversion recovery (SPAIR), frequency-selective fat saturation (FatSat), water-selective excitation or the Dixon technique]. Each one is based on different physical phenomena,[4–6] and previous studies have described their variable efficiency in lesion detection, and ADC estimates.[7–10]

Given that the available techniques are not equally robust to the static magnetic field (B0) and radiofrequency magnetic field (B1) inhomogeneities, it is important to compare their performance on breast DWI at 3 T. Previous studies[7,8,11] have used different techniques for fat suppression: Bogner et al.[7] used STIR, whereas Peters et al.[8] and El Khouli et al.[11] used SPAIR, which makes direct comparisons difficult. For example, comparing results previously obtained by the present authors' group using a SPAIR-based sequence[12] with those reported by Bogner et al.[7] using STIR (b-values 50 and 1000 s/mm^2 in both cases), similar ADC values were obtained for malignant and normal glandular tissue, but not for benign lesions, which could potentially be related to differences in fat-suppression efficiency.

Echo planar imaging (EPI) is a fast acquisition technique commonly used in breast DWI. It enables high imaging speed at the cost of being prone to chemical shift artefacts and geometric distortions.[13] A common strategy to decrease these artefacts is to use parallel imaging (PI), an image reconstruction technique that makes use of sensitivity differences between different coil channels to perform spatial encoding, enabling a reduction in the number of phase-encoding steps. This in turn leads to a shorter readout window and hence reduced geometric distortion in the images.[14] Another study developed by the present authors comparing DWI-STIR and -SPAIR at 3 T including PI[15] [*in press*] revealed similar contrast-to-noise ratio (CNR) and signal-to-noise ratio (SNR) except for benign lesions, and comparable ADC values for benign and malignant lesions.

However, some authors reported a decrease in SNR and CNR with PI as the echo time (TE) shortening achievable with PI can be insufficient to compensate for the g-factor noise penalty, which depends on the coil geometry and reflects the difference in sensitivity of the available channels along the phase encode direction.[16,17] Given that the present DWI sequence includes higher b-values (b = 2000 and 3000 s/mm^2) the decision was made to exclude PI to gain SNR. Thus, the purpose of the present study was to compare quantitatively DWI-STIR and -SPAIR when no PI is used regarding SNR and CNR, fat-suppression uniformity, and ADC quantification for lesion differentiation and characterization in the clinical setting.

Materials and methods

Patients and lesions

The present study is included in a wider investigation focusing on the application of DWI to study breast lesions, for which approval has been obtained from the institutional review board (code CES 276/13). This prospective study was performed on women with clinical indication for breast MRI. Written informed consent was obtained from all patients.

Women were excluded from this study if they (1) had undergone chemotherapy or radiotherapy 24 months prior to the MRI examination (three women with four lesions); (2) had had surgery <2 years before; (3) had completed hormone-replacement therapy within 24 months of the examination; (4) had breast implants; and (5) only one fat-saturation technique was performed (two women with two lesions).

Inclusion criteria for lesion analysis were (1) a minimum size of 0.7 cm in the dynamic contrast-enhanced (DCE) sequence; (2) a definitive outcome obtained through histology (core needle biopsy or excised surgery), and/or a minimum 2 year follow-up by mammography, ultrasound, or MRI.

All premenopausal women performed breast MRI examination between the 7th and 14th day of their menstrual cycle to diminish enhancement of normal glandular tissue after contrast medium injection.[18] For women who had undergone biopsy before MRI examination, a minimum interval of 10 days prior to the MRI examination was enforced to minimize signal intensity changes due to potential haemorrhage and/or oedema.

In the benign lesions group, only solid lesions were included in the ADC calculation. Cystic lesions were excluded as their high ADC would bias ADC estimates.

Acquisition protocol

All MRI examinations were performed using a 3 T system (Magnetom Tim Trio®, Siemens, Erlangen, Germany) equipped with a four-channel dedicated breast radiofrequency (RF) coil (Invivo Corporation). Patients were examined in a resting prone position with the total volume of the breast in the coil compartment.

The imaging protocol included axial T2-weighted (W) turbo spin-echo (TSE); sagittal three-dimensional (3D) T1W fast low-angle shot (FLASH) without fat suppression; sagittal T2W TSE STIR; sagittal DWI; axial 3D T1W FLASH DCE with SPAIR for fat suppression, acquired after gadobenate dimeglumine injection (MultiHance; Bracco, Milan, Italy), and a sagittal 3D T1W FLASH post-contrast

sequence with water-selective excitation as the fat-suppression technique.

Before the DCE pulse sequence, two DW single-shot spin-echo EPI (DW-SS-SE-EPI) sequences with either STIR or SPAIR as the fat-suppression module were carried out. The DW images were acquired in the sagittal plane for each breast, with the sensitizing diffusion gradients applied along the *x*, *y* and *z* directions to generate three-scan-trace images. Volume shimming adjusted to the field-of-view (FOV) was performed to improve magnetic field homogeneity. Table 1 describes the details of DWI-STIR and -SPAIR.

A minimum TE of 106 (and 108 ms) had to be applied to include b-values 2000 and 3000 s/mm^2. These were used to explore the non-Gaussian distribution of diffusion.[19] Considering that at 3 T a transverse relaxation time T2 of 71 ± 6 ms has been reported for normal fibroglandular tissue,[20] extending the TE from 78 to 106 and 108 ms, respectively for SPAIR and STIR, resulted in a signal loss of 34%. This was compensated for by increasing the number of excitations (NEX) to 3, resulting in a final SNR improvement of 17% and 14%, for SPAIR and STIR, respectively.

To simplify the analysis, only the pair of DWI with b-values of 50 and 1000 s/mm^2 and derived ADC was included in the present study. This choice was based on a previous study developed by the authors to determine the best pair of b-values for breast lesion differentiation.[12]

Image analysis

The image-processing platform of the MRI machine and the software provided by the manufacturer were used to analyse the images [Siemens Medical Systems, work in progress (WIP) version 17A]. The same experienced breast imaging radiologist, with 7 years of experience, reported all the examinations. Lesions were evaluated according to their morphological and kinetic characteristics, as described by the American College of Radiology (ACR) Breast Imaging Reporting and Data System-MRI (BIRADS-MRI).[21] Lesion size was measured using the ruler function on DCE images and considering its maximum diameter.

Table 1
Main imaging parameters for diffusion-weighted imaging short tau inversion recovery (DWI-STIR) and spectral adiabatic inversion recovery (SPAIR).

Parameters	DWI	
Sequence	SS-SE-EPI	SS-SE-EPI
Fat suppression	STIR	SPAIR
Orientation	Sagittal	Sagittal
TR/TE (ms)	4900/108	4900/106
TI (ms)	240	–
FOV (mm^2)	250 × 250	250 × 250
Matrix (pixels)	84 × 128	84 × 128
Phase encoding direction	head-to-feet	head-to-feet
Slice thickness (mm)	5	5
Voxel (mm^3)	2 × 2 × 5	2 × 2 × 5
NEX	3	3
Bandwidth (Hz/pixel)	1628	1628
Scan time (min)	5:58	5:58
b-values (s/mm^2)	50, 200, 400, 600, 800, 1000, 2000 and 3000	50, 200, 400, 600, 800, 1000, 2000 and 3000

DWI, diffusion-weighted imaging; FOV, field of view; NEX, number of excitations; SPAIR, spectral adiabatic inversion recovery; SS-SE-EPI, single-shot spin-echo echo planar imaging; STIR, short tau inversion recovery; TI, inversion time; TR/TE, repetition time/echo time.

DWI datasets were retrospectively analysed by two radiological researchers in consensus (with 6 and 11 years of experience in breast MRI). At the time of interpretation, both were blinded to the final histological results. To identify lesions in the DW images, the conventional MRI report description and the visual inspection of the T1W, T2W, the subtracted early DCE, and the post-contrast images were used as reference for both fat-saturation techniques.

Fixed, circular region of interest (ROI) of 0.25 cm^2 were used to measure the signal intensity in lesions, normal glandular tissue, and noisy background (along the readout direction to avoid including EPI ghosts, which are image artefacts that can appear along the phase-encoding direction of the image). The same area and section were selected for both fat-saturation techniques when drawing the ROIs. These were defined at b = 1000 s/mm^2, in the section that showed the maximum dimension and best definition of the lesion and its margins within the area of highest hyperintensity. Care was taken to avoid areas of necrosis or hyperintensity due to T2 shine-through effect, through visual comparison with T1W and T2W images. The ROIs were then copied to the corresponding section at b = 50 s/mm^2.

In women with unilateral lesions, normal glandular tissue signal intensity was measured in the central section of the contralateral breast at b = 1000 s/mm^2, avoiding areas of fatty tissue, and then copied to b = 50 s/mm^2.

For both fat-saturation techniques, the analysis of SNR, CNR, and suppression uniformity was performed at b = 1000 s/mm^2 for lesions and normal glandular tissue.

SNR was calculated using the equation[22]

$$SNR = SI_{lesion} \Big/ SD_{background},$$

where SI_{lesion} is the mean signal intensity in the lesion and $SD_{background}$ is the average of the background noise in the air. To estimate background noise, the section that better depicted the lesion was chosen, and measurements were performed placing three ROIs of 0.25 cm^2 in the air; 1 cm above, below and anterior to the nipple. Background noise was calculated as the average of the standard deviation (SD) of the three ROIs measurements as reported by Woodhams et al.[23]

To estimate the CNR between lesion and normal glandular tissue, signal intensity of normal tissue was measured in the same side as the lesion, and the CNR estimated with the following equation.

$$CNR = (SI_{lesion} - SI_{normal\ tissue}) \Big/ SD_{background},$$

where SI_{lesion} is the signal intensity of the lesion and $SI_{normal\ tissue}$ is the signal intensity of the normal fibroglandular tissue in the same breast, $SD_{background}$ is the average of the SD in the background signal.

For each DWI technique, fat-saturation uniformity was assessed considering the average of the SD of the signal intensity measured in the normal glandular tissue, as

although these measurements are affected by noise (higher SNR should lead to lower SD), heterogeneous fat saturation should lead to higher SD within the ROIs.

For both techniques, ADC maps were estimated for each lesion and for normal glandular tissue with b-values 50 and 1000 s/mm^2, using the equation

$$ADC = \frac{ln[S(b_1)] - ln[S(b_2)]}{b_2 - b_1}$$

where *S(b)* represents the signal intensity measured for each b-value.

Statistical analysis

To characterize the study population, a descriptive analysis was performed. The Kolmogorov–Smirnov test was used to verify the distribution of the data. For each technique and by tissue type, mean values of SNR, CNR, uniformity of fat suppression, and ADCs were calculated. The differences were evaluated with the Mann–Whitney test and the independent samples Student's *t*-test depending on the probability distribution of the data.

Comparison between DWI-STIR and -SPAIR regarding image quality parameters and ADC was performed using the Wilcoxon signed-rank test or the paired samples Student's *t*-test. Spearman's and Pearson's tests were used to evaluate the correlation in measurements between DWI-STIR and -SPAIR.

For each fat-suppression technique, the ADC cut-off point was calculated, considering Youden statistics and the minimal distance between the receiver operating characteristics (ROC) curves and the ideal point of coordinates (0, 1) where both the sensitivity and specificity have a maximum value of 1. The diagnostic performance for each technique in lesion discrimination was evaluated, including the use of the McNemar test.

All analyses were performed using the PASW Statistics V21 software. A *p*-value of <0.05 was considered to indicate a significant difference.

Results

Patients and lesion characteristics

Ninety-two women (mean ± standard deviation age of 48 ± 12 years; range 21–78 years) with 114 lesions were successfully scanned with DWI-STIR and -SPAIR. Thirty-seven women were post-menopausal. One hundred and four lesions were mass (91.2%) and 10 non-mass lesions (8.8%). Among the 114 lesions, 74 were classified as malignant and 40 as benign. Histological results were obtained for 99 lesions by biopsy and/or surgery. Mean size for benign lesions was 13.±9 mm, whereas for malignant lesions it was 25 ± 15 mm. Significant differences in size by lesion type were found ($p < 1 \times 10^{-4}$). For malignant lesions histological results were nine ductal carcinoma *in situ*; three lobular carcinoma *in situ*; 35 invasive ductal carcinoma; 18 invasive lobular carcinoma; one mucinous carcinoma; eight classified as others malignant lesions not otherwise specified (NOS).

For 25 benign lesions, histological analysis revealed 12 fibroadenomas; six epithelial proliferative lesions; two papillomas; one hamartoma; four other benign, namely one sclerosing adenosis, one fibrocystic change, two epithelial proliferative lesions with miofibroblastic proliferation and infiltrative inflammation.

For eight benign lesions (five were fibroadenomas, two were fibrocystic change, and one was a sclerosing adenosis) histological results were available prior to the study. These lesions were diagnosed in women with BRCA mutation that perform annual MRI follow-up. The remaining seven benign lesions were cysts identified by ultrasound and DWI-MRI, but which were excluded from the ADC analysis.

Fig 1 illustrates an invasive ductal carcinoma in the left breast of a 38-year-old woman. MRI included STIR (a) dynamic (b) and DW images using -STIR (c,d) and -SPAIR (e,f) (b1000 s/mm^2 and ADC maps, respectively).

Comparison between DWI-STIR and -SPAIR

Differences in mean ADC values, SNR, CNR, and saturation uniformity for each fat-suppression technique and comparison between DWI-STIR and -SPAIR, as well as correlation between measurements are presented in Table 2.

Mean ADC values were higher for DWI-STIR. For both DWI-STIR and -SPAIR mean ADC values of malignant lesions were lower (1.18 ± 0.42; 1.11 ± 0.04 × 10^{-3} mm^2/s) than benign lesions (1.92 ± 0.45; 1.80 ± 0.38 × 10^{-3} mm^2/s), with significant differences between them ($p < 1 \times 10^{-4}$; $p < 1 \times 10^{-4}$), respectively.

DWI-STIR showed no differences between benign and malignant lesions for SNR, CNR or fat-suppression uniformity ($p = 0.588$; $p = 0.287$; $p = 0.701$, respectively). For DWI-SPAIR there were also no differences in SNR, CNR, and fat-suppression uniformity between benign and malignant lesions ($p = 0.636$; $p = 0.252$; $p = 0.549$). Fat-suppression uniformity was better for DWI-STIR than for -SPAIR (0.73 ± 0.47 versus 1.42 ± 0.93).

Comparison between fat-suppression techniques showed significant differences in ADC values for benign ($p = 0.013$) and malignant lesions ($p = 0.001$), with high correlation between measurements for lesion type (benign: $r = 0.785$; $p < 1 \times 10^{-4}$ and malignant: $r = 0.769$; $p < 1 \times 10^{-4}$). ADC values for normal glandular tissue were similar ($p = 0.072$), with a strong correlation between measurements ($r = 0.813$; $p < 1 \times 10^{-4}$).

Higher SNR was found for DWI-SPAIR than -STIR, with significant differences for benign ($p = 0.017$), malignant ($p = 0.001$) and normal glandular tissue ($p = 0.035$), with high correlation for benign ($r = 0.754$; $p < 1 \times 10^{-4}$) and malignant lesions ($r = 0.606$; $p < 1 \times 10^{-4}$). For normal glandular tissue, no correlation was found between DWI-STIR and -SPAIR ($r = 0.047$; $p = 0.781$).

CNR was also higher for DWI-SPAIR than -STIR, regardless of lesion type, with significant differences in CNR values for malignant ($p = 0.005$) and no differences for benign lesions ($p = 0.063$). Also, no correlations were observed for

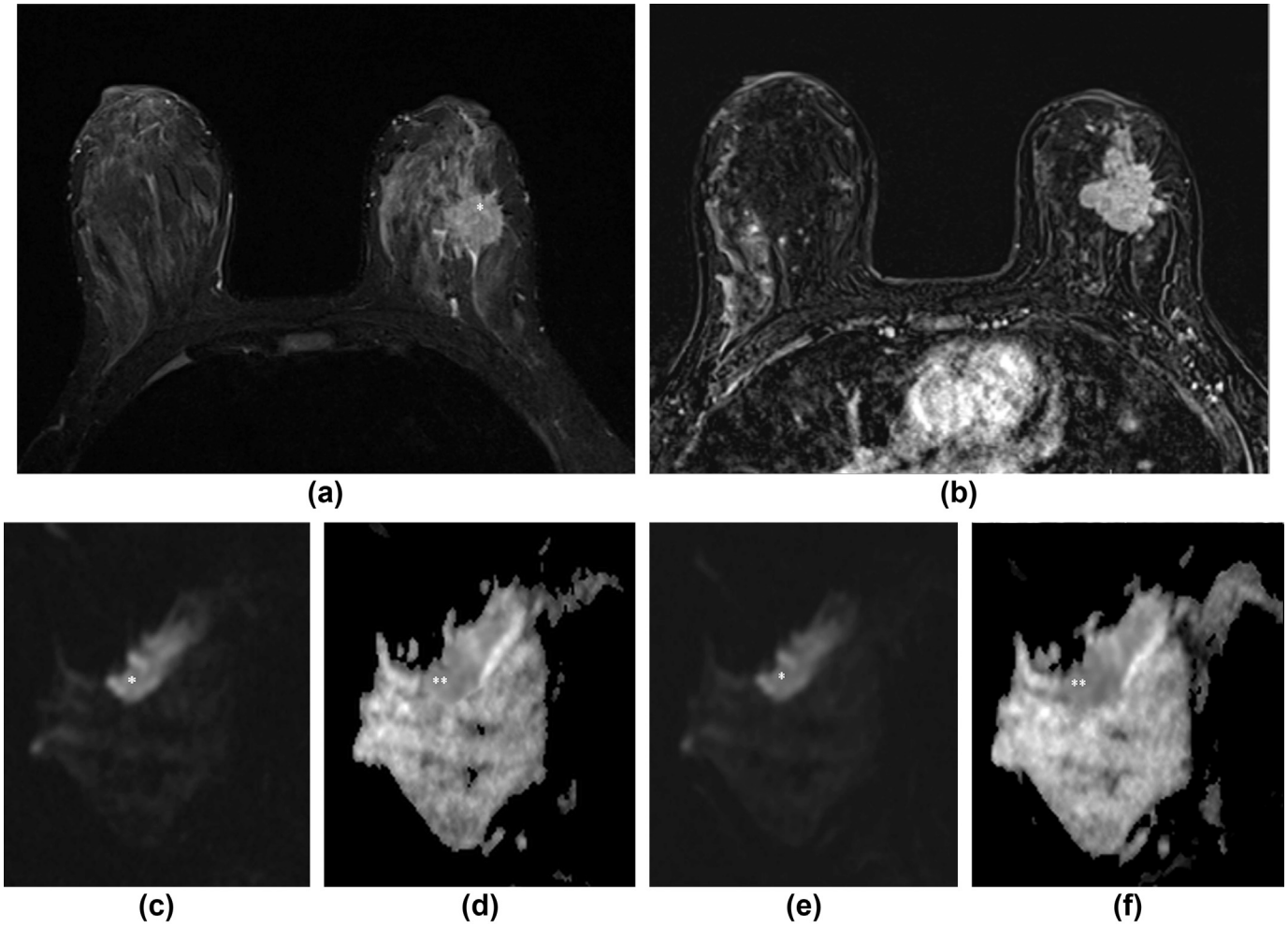

Figure 1 Thirty-eight year-old woman with grade III invasive ductal carcinoma, with *in situ* component. Axial bilateral STIR (a) and dynamic sequence with clear definition of irregular lesion border (b), and DWI acquisitions [DWI-STIR b = 1000 s/mm^2/ADC map (c,d); DWI-SPAIR b = 1000 s/mm^2/ADC map (e,f)]. The lesion is highly cellular, with increased signal intensity on STIR and on both DWI sequences (*), with the respective low signal intensity on the ADC maps (**).

CNR between techniques for malignant ($r = 0.399$; $p = 0.073$) or benign ($r = 0.679$; $p = 0.094$) lesions.

Comparison between DWI-STIR and -SPAIR in fat-suppression uniformity presented significant differences for benign ($p < 1 \times 10^{-4}$), malignant ($p < 1 \times 10^{-4}$) and all (benign plus malignant) lesions ($p < 1 \times 10^{-4}$). Also, no correlations were observed between techniques for benign ($r = 0.224$; $p = 0.282$) and malignant ($r = 0.282$; $p = 0.061$) lesions, although a weak and significant correlation was observed when considering all lesions together ($r = 0.278$; $p = 0.020$).

Diagnostic performance of DWI-STIR and -SPAIR

To assess the influence of the fat-saturation technique in lesion discrimination, ROC analysis was performed to calculate the optimal ADC thresholds for DWI-STIR and -SPAIR (Fig 2). The area under the curve (AUC) was higher for DWI-SPAIR (89.2%; 95% CI: 83.5–94.9) than -STIR (87.7%; 95% CI: 81.5–93.9). The ADC threshold for discriminating benign from malignant lesions was 1.42×10^{-3} mm^2/s and 1.46×10^{-3} mm^2/s for DWI-STIR and -SPAIR, respectively. Lesions with mean ADC values below the respective threshold for each fat-saturation technique were classified as malignant. Based on those ADCs thresholds, diagnostic performance is presented in Table 3.

DWI-SPAIR showed absolute higher sensitivity in lesion discrimination than -STIR. For DWI-SPAIR, false-positive cases were four fibroadenomas, one sclerosing adenosis, one papilloma, two epithelial proliferative changes, one of which presented miofibroblastic proliferation and infiltrative inflammation. False-negative cases were two ductal carcinoma *in situ*, five extensively spread invasive lobular carcinomas, three invasive ductal carcinomas, and one lesion classified as NOS with signet ring cell and mucin.

DWI-STIR displayed two less false-positive cases: three fibroadenomas, one papilloma, two epithelial proliferative lesions, one of which presented miofibroblastic proliferation and infiltrative inflammation. These are the same lesions misclassified by DWI-SPAIR. On the other hand, DWI-STIR revealed four more false-negative cases than DWI-SPAIR, namely two invasive lobular carcinomas, one

Table 2
Mean ± standard deviation apparent diffusion coefficient (ADC) values and image quality parameters for each fat-saturation technique and comparison between DWI-STIR and -SPAIR.

	DWI-STIR (Mean ± SD)	Benign versus Malignant STIR p-value[a]	DWI-SPAIR (Mean ± SD)	Benign versus Malignant SPAIR p-value[b]	STIR versus SPAIR p-value[c]	STIR-SPAIR correlation (r_S)[d]
ADC ($\times 10^{-3}$ mm^2/s)						
Benign	1.92 ± 0.45	$<1 \times 10^{-4}$	1.80 ± 0.38	$<1 \times 10^{-4}$	0.013	0.785 ($p < 1 \times 10^{-4}$)
Malignant	1.18 ± 0.42		1.11 ± 0.04		0.001	0.769 ($p < 1 \times 10^{-4}$)
Normal tissue	1.86 ± 0.41	–	1.79 ± 0.38	–	0.072	0.813 ($p < 1 \times 10^{-4}$)
SNR						
Benign	59.8 ± 37.4	0.588	76.6 ± 57.7	0.636	0.017	0.754 ($p < 1 \times 10^{-4}$)
Malignant	62.3 ± 32.8		81.8 ± 48.7		0.001	0.606 ($p < 1 \times 10^{-4}$)
Normal tissue	26.1 ± 19.8	–	33.4 ± 19.4	–	0.035	0.047 ($p = 0.781$)
CNR						
Benign	53.2 ± 43.6	0.287	70.3 ± 50.0	0.252	0.063	0.679 ($p = 0.094$)
Malignant	31.9 ± 20.0		57.6 ± 42.0		0.005	0.399 ($p = 0.073$)
Uniformity						
Benign	0.70 ± 0.38	0.701	1.50 ± 0.98	0.549	$<1 \times 10^{-4}$	0.224 ($p = 0.282$)
Malignant	0.74 ± 0.52		1.37 ± 0.91		$<1 \times 10^{-4}$	0.282 ($p = 0.061$)
All lesions	0.73 ± 0.47	–	1.42 ± 0.93	–	$<1 \times 10^{-4}$	0.278 ($p = 0.020$)

ADC, apparent diffusion coefficient; CNR, contrast-to-noise ratio; DWI, diffusion-weighted imaging; SD, standard deviation, SNR, signal-to-noise ratio; SPAIR, spectral adiabatic inversion recovery; STIR, short tau inversion recovery.
[a] Differences in ADC values and image-quality parameters between tissue types for DWI-STIR.
[b] Differences in ADC values and image-quality parameters between tissue types for DWI-SPAIR.
[c] Comparison between DWI-STIR and -SPAIR regarding ADC values and image-quality parameters.
[d] Spearman's rank correlation between DWI-STIR and -SPAIR for ADC values and image-quality parameters.

invasive ductal carcinoma with *in situ* component, and one mucinous carcinoma.

The positive and negative predictive values for DWI-STIR and -SPAIR were 90.8% and 88.7% and 69.4% and 74.4%, respectively.

Accuracy in lesion discrimination was 81.6% for DWI-STIR and 83.3% for DWI-SPAIR. Regarding the comparison in diagnostic performance, no differences were observed between DWI-STIR and -SPAIR ($p = 0.096$). The comparison between diagnostic performance and histological results also showed no differences for DWI-SPAIR ($p = 0.481$) but significant differences were observed for DWI-STIR ($p = 0.023$).

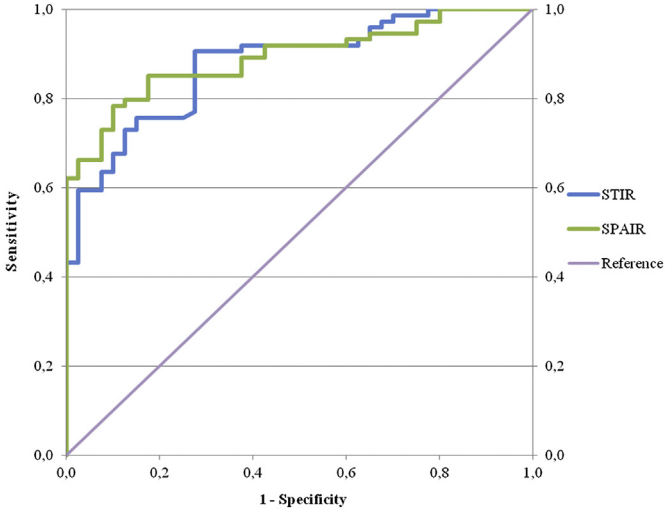

Figure 2 ROC curves used to differentiate benign and malignant lesions based on mean ADC values for each fat suppression technique, namely DWI-STIR and -SPAIR.

Discussion

Achieving adequate elimination of the lipid signal is challenging, especially at magnetic field strengths ≥3 T due to increased susceptibility artefacts, image ghosting, and larger chemical shifts that can be present when compared to 1.5 T.[14] To address these issues while preserving image quality, the use of an adequate fat-suppression method is

Table 3
Diagnostic performance of DWI-STIR and -SPAIR in lesion discrimination.

	DWI-STIR	DWI-SPAIR
ADC cut-off ($\times 10^{-3}$ mm^2/s)	1.42	1.46
False positive	6	8
False negative	15	11
True positive	59	63
True negative	34	32
Sensitivity, 95% CI (%)	79.7 [70.6; 88.9]	85.1 [77.0; 93.2]
Specificity, 95% CI (%)	85 [73.9; 96.1]	80 [67.6; 92.4]
Positive predictive value, 95% CI (%)	90.8 [83.7; 97.8]	88.7[81.4; 96.1]
Negative predictive value, 95% CI (%)	69.4 [56.5; 82.3]	74.4 [61.4; 87.5]
Accuracy, 95% CI (%)	81.6 [74.5; 88.7]	83.3 [76.5; 90.2]
AUC, 95% CI (%)	87.7 [81.5; 93.9]	89.2 [83.5; 94.9]
Diagnostic performance McNemar test (p-value)[a]	0.023	0.481

ADC, apparent diffusion coefficient; AUC, area under the curve; CI, confidence interval.
[a] The McNemar test was used to compare the diagnostic performance of DWI-STIR and SPAIR methods regarding histological results. Also, the comparison of the diagnostic performances of DWI-STIR and SPAIR methods between themselves held a $p = 0.096$.

essential to mitigate image artefacts and promote adequate SNR and CNR.[24] Also, unsuppressed fat signal interferes with the diffusivity characteristics of the underlying tissue, resulting in underestimation of ADC values.[25,26]

Different fat-suppression techniques are available for breast DWI.[27] In the present study DWI-STIR and -SPAIR were investigated for breast DWI at 3 T. These fat-saturation techniques were chosen because of their physical characteristics and robustness to deal with B0 and B1 inhomogeneities that are more pronounced at higher fields.[14]

Previous investigations focusing on this subject were performed mainly at 1.5 T, and some controversy still exists regarding the impact of the fat-suppression module on image quality and ADC quantification.[5,9,28,29] Differences in DWI pulse sequence parameters or the use of different fat-suppression methods prevent a direct comparison between studies. Using PI, lower SNR and CNR had been reported by Jin et al.[16] To isolate the effect of the fat-suppression technique, all other acquisition parameters were kept as constant as possible.

DWI-SPAIR showed higher SNR and CNR than -STIR. SNR results are in agreement with a previous study developed by Baron et al.,[27] who found a slightly higher SNR for DWI-SPAIR than -STIR in normal glandular tissue, without significant differences. The most likely explanation for these findings is that STIR is based on a non-selective 180° radiofrequency inversion pre-pulse that inverts not only lipids but also water spins; this leads to reduced water signal due to incomplete magnetization recovery, resulting in lower SNR. Nonetheless, STIR has the advantage of being largely immune to B0 inhomogeneities.[30] Conversely, DWI-SPAIR only inverts spins centred at the precessional frequency of lipids, allowing the overall water signal to be unchanged and higher SNR to be obtained.[31] As an advantage, SPAIR is relatively indifferent to B1 inhomogeneities due to the use of adiabatic inversion pulses (RF pulses with variable frequency).[28,32] Significant differences were found in the CNR values of malignant lesions between DWI-SPAIR and -STIR, indicating that lesion visualization may be hampered in DWI-STIR, although in the present series all lesions were detected using either saturation technique.

Fat-suppression uniformity was better for DWI-STIR when compared to -SPAIR for all the tissues analysed. One explanation for the incomplete suppression of the lipid signal lies in the fact that SPAIR is based on spectrally selective pulses that only suppress the contribution from the largest lipid peak at a resonance frequency of approximately 3.5 ppm relative to water.[4] Minor lipid peaks at different resonance frequencies[33] remain unsuppressed and still contribute to the final signal intensity.[34,35] Additionally, STIR seems to produce a more spatially homogeneous suppression throughout the image. Given that the acquisition parameters are very similar for both DW sequences, the differences found on the image-quality parameters can be attributed to the fat-suppression module applied.

Differentiation and characterization of benign and malignant lesions is based on their ADC. When comparing the present mean ADC values for benign and malignant lesions and normal glandular tissue with previous studies that also did not apply PI, results are within the same range.[7,9] The lower ADC values found with DWI-SPAIR when compared to -STIR, for both benign and malignant lesions are compatible with incomplete lipid suppression with -SPAIR. As the lipid signals are spatially mapped onto an incorrect location, regions of lesion/parenchyma may be contaminated, and the ADC estimates affected. As lipids have been reported to have low ADC values[5] if their signal is not completely eliminated, a lower ADC will be measured as found here with DWI-SPAIR. The results of the present study indicate significant differences in the ADCs and image-quality parameters, except for ADCs in normal glandular tissue and CNR in benign lesions. Furthermore, a high correlation in measurements between fat-suppression techniques was found and the ADCs were monotonically related, which means that the contribution of the lipid signals, although varying according to the fat suppression used, affects each individual lesion in a similar way.

Theoretically, the ADC value in a lesion without adipose tissue should be exactly the same for both fat-saturation techniques. However, lesions present heterogeneous environments including variable fat content, and therefore, differences in ADC estimates were expected. The results of the present study confirm the presence of fat content in lesions, as translated by the difference in mean ADC values using STIR and SPAIR. Also, the percentual difference of these ADC values for benign (6.7%) and malignant lesions (6.3%) are observed to be larger than for normal tissue (3.9%), which suggests that lesions have variable fat content. These results also agree with a previous study that reported higher fat content in benign compared to malignant lesions.[36]

The diagnostic performance of breast DWI relies on the individual ADC value and established thresholds for lesion discrimination.[37] In a recent meta-analysis ADC cut-off values to differentiate benign from malignant lesions have been reported ranging from 1.1×10^{-3} to 1.6×10^{-3} mm^2/s.[38] The thresholds used in the present study are in the range of those previously reported for b-values 0 and 1000 s/mm^2 (1.46×10^{-3} mm^2/s for DWI-SPAIR and 1.42×10^{-3} mm^2/s for DWI-STIR). Assuming the individual ADC threshold, DWI-SPAIR showed higher sensitivity, accuracy, and an AUC slightly higher than -STIR. However, specificity was higher for DWI-STIR than -SPAIR (85% versus 80%). The comparison between fat-suppression methods revealed similar diagnostic performance ($p = 0.096$). Nevertheless, when each fat suppression was compared with the reference standard adopted in breast lesion classification, DWI-SPAIR seems be preferable to -STIR.

False-positive and -negative cases were found for both fat-saturation methods. Six of the false-positive cases were misclassified by both techniques, namely three fibroadenoma, one papilloma, and two epithelial proliferative lesions. Additionally, DWI-SPAIR failed to classify two additional lesions (one fibroadenoma and one sclerosing adenosis). Different causes could explain these results, such as the presence of fibrosis and increased cellularity and/or increased cell proliferation, which restricts water diffusivity and lowers the ADC values.

Eleven of the false-negative cases were the same for both fat-saturation methods (two ductal carcinoma *in situ*, five invasive lobular carcinoma, three invasive ductal carcinoma, and one as malignant lesion NOS). However, DWI-STIR showed four more false-negative cases than -SPAIR (two highly spread invasive lobular carcinoma, one invasive ductal carcinoma with *in situ* component, and one mucinous carcinoma). Other groups reported similar false-negative results.[39,40] A possible explanation for these additional misclassified lesions in STIR versus SPAIR could be related to incomplete fat suppression in the former case. As lipids present a lower ADC compared to water, the overall ADC would be lower.

Although artefacts were not quantified, they appeared to be more prevalent on DWI-SPAIR than -STIR. To minimize artefacts through the image and field inhomogeneities, a reduced FOV, automatic first-order shimming, and manual adjustment of water and fat frequencies were used.

The present study has some limitations. The number of benign lesions is smaller than malignant lesions, which could bias the reported positive and negative predictive values. Also, using 3 T MRI, some authors[8,10] reported to be able to detect lesions with 4 and 3 mm sizes in DW images. As the lesion size in the present sample was $\geq$7 mm, future work should test the impact of both fat-saturation techniques in the detection of smaller lesions. Additionally, lesion demarcation was performed by two researchers in consensus, when in the clinical practice only one researcher would do it.

In conclusion, image quality, suppression uniformity, mean ADC values, and the established thresholds used for lesion differentiation are influenced by the fat-suppression technique. Both techniques present similar AUC, which means that either could be used in the clinical setting. Nonetheless, the DWI-SPAIR technique showed a diagnostic performance more similar to histology than the -STIR technique, thus suggesting that the -SPAIR fat-suppression technique may be overall more accurate.

Conclusion

- The fat saturation technique used in breast DWI influences image quality.
- Fat suppression uniformity was better for DWI-STIR than -SPAIR.
- ADC quantification and cut-off values depend on the fat suppression used.
- Diagnostic performance between DWI-STIR and -SPAIR was not significantly different.
- DWI-SPAIR seems to be more accurate using as reference histological results.

References

1. Guo Y, Cai YQ, Cai ZL, et al. Differentiation of clinically benign and malignant breast lesions using diffusion-weighted imaging. *J Magn Reson Imaging* 2002;**16**:172–8.
2. Belli P, Costantini M, Bufi E, et al. Diffusion-weighted imaging in breast lesion evaluation. *Radiol Med* 2010;**115**:51–69.
3. Lo GG, Ai V, Chan JK, et al. Diffusion-weighted magnetic resonance imaging of breast lesions: first experiences at 3 T. *J Comput Assist Tomogr* 2009;**33**:63–9.
4. Bley TA, Wieben O, François CJ, et al. Fat and water magnetic resonance imaging. *J Magn Reson Imaging* 2010;**31**:4–18.
5. Partridge SC, Singer L, Sun R, et al. Diffusion-weighted MRI: influence of intravoxel fat signal and breast density on breast tumor conspicuity and apparent diffusion coefficient measurements. *Magn Reson Imaging* 2011;**29**:1215–21.
6. Ma J. Dixon techniques for water and fat imaging. *J Magn Reson Imaging* 2008;**28**:543–58.
7. Bogner W, Gruber S, Pinker K, et al. Diffusion-weighted MR for differentiation of breast lesions at 3.0T: how does selection of diffusion protocols affect diagnosis? *Radiology* 2009;**253**:341–51.
8. Peters NH, Vincken KL, Van den Bosch MA, et al. Quantitative diffusion weighted imaging for differentiation of benign and malignant breast lesions: the influence of the choice of b-values. *J Magn Reson Imaging* 2010;**31**:1100–5.
9. Wenkel E, Geppert C, Schulz-Wendtland R, et al. Diffusion weighted imaging in breast MRI: comparison of two different pulse sequences. *Acad Radiol* 2007;**14**:1077–83.
10. Matsuoka A, Minato M, Harada M, et al. Comparison of 3.0-and 1.5-Tesla diffusion-weighted imaging in the visibility of breast cancer. *Radiat Med* 2008;**26**:15–20.
11. El Khouli RH, Jacobs MA, Mezban SD, et al. Diffusion-weighted imaging improves the diagnostic accuracy of conventional 3.0-T breast MR imaging. *Radiology* 2010;**256**:64–73.
12. Nogueira L, Brandão S, Matos E, et al. Diffusion-weighted imaging: determination of the best pair of b-values to discriminate breast lesions. *Br J Radiol* 2014;**87**:20130807.
13. Skare ST, Bammer R. EPI-based pulse sequences for diffusion tensor MRI. In: Jones DK, editor. *Diffusion MRI — theory, methods and applications*. Oxford: University Press; 2011. p. 182–202.
14. Rakow-Penner R, Hargreaves B, Glover G, et al. Breast MRI at 3T. *Appl Radiol* 2009;**38**:6–13.
15. Brandão S, Nogueira L, Matos E, et al. Fat suppression techniques (STIR vs. SPAIR) on diffusion weighted imaging of breast lesions at 3.0T: preliminary experience. *Radiol Med* 2014. In press.
16. Jin G, An N, Jacobs MA, et al. The role of parallel diffusion-weighted imaging and apparent diffusion coefficient (ADC) map values for evaluating breast lesions: preliminary results. *Acad Radiol* 2010;**17**:456–63.
17. Heidemann RM, Seiberlich N, Griswold MA, et al. Perspectives and limitations of parallel MR imaging at high field strengths. *Neuroimaging Clin N Am* 2006;**16**:311–20.
18. Partridge SC, McKinnon GC, Henry RG, et al. Menstrual cycle variation of apparent diffusion coefficients measured in the normal breast using MRI. *J Magn Reson Imaging* 2001;**14**:433–8.
19. Nogueira L, Brandão S, Matos E, et al. Application of the diffusion kurtosis model for the study of breast lesions. *Eur Radiol* 2014;**24**:1197–203.
20. Edden RA, Smith SA, Barker PB. Longitudinal and multi-echo transverse relaxation times of normal breast tissue at 3 Tesla. *J Magn Reson Imaging* 2010;**32**:982–7.
21. Morris EA, Comstock CE, Lee CH, et al. ACR BI-RADS® magnetic resonance imaging. In: *ACR BI-RADS® atlas, breast imaging reporting and data system*. Reston, VA: American College of Radiology; 2013. p. 125–43.
22. Kaufman K, Kramer DM, Crooks LE, et al. Measuring signal-to-noise ratios in MR imaging. *Radiology* 1989;**173**:265–7.

23. Woodhams R, Inoue Y, Ramadan S, et al. Diffusion-weighted Imaging of the breast: comparison of b-values 1000 s/mm^2 and 1500 s/mm^2. *Magn Reson Med Sci* 2013;**12**:229–34.
24. Thomassin-Naggara I, De Bazelaire C, Chopier J, et al. Diffusion-weighted MR imaging of the breast: advantages and pitfalls. *Eur J Radiol* 2013;**82**:435–43.
25. Ababneh ZQ, Beloeil H, Berde CB, et al. *In vivo* lipid diffusion coefficient measurements in rat bone marrow. *Magn Reson Imaging* 2009;**27**:859–64.
26. Qiao Y, Ronen I, Viereck J, et al. Identification of atherosclerotic lipid deposits by diffusion-weighted imaging. *Arterioscler Thromb Vasc Biol* 2007;**27**:1440–6.
27. Baron P, Dorrius MD, Kappert P, et al. Diffusion-weighted imaging of normal fibroglandular breast tissue: influence of microperfusion and fat suppression technique on the apparent diffusion coefficient. *NMR Biomed* 2010;**23**:399–405.
28. Kazama T, Nasu K, Kuroki Y, et al. Comparison of diffusion-weighted images using short inversion time inversion recovery or chemical shift selective pulse as fat suppression in patients with breast cancer. *Jpn J Radiol* 2009;**27**:163–7.
29. Kuroki Y, Nasu K. Advances in breast MRI: diffusion-weighted imaging of the breast. *Breast Cancer* 2008;**15**:212–7.
30. Delfaut EM, Beltran J, Johnson G, et al. Fat suppression in MR imaging: techniques and pitfalls. *RadioGraphics* 1999;**19**:373–82.
31. Koh DM, Takahara T, Imai Y, et al. Practical aspects of assessing tumors using clinical Diffusion-weighted imaging in the body. *Magn Reson Med Sci* 2007;**6**:211–4.
32. Murtz P, Krautmacher C, Traber F, et al. Diffusion-weighted whole-body MR Imaging with background body signal suppression: a feasibility study at 3.0 Tesla. *Eur Radiol* 2007;**7**:3031–7.
33. Singer S, Sivaraja M, Souza K, et al. ^{1}H-NMR detectable fatty acyl chain unsaturation in excised leiomyosarcoma correlates with grade and mitotic activity. *J Clin Invest* 1996;**98**:244–50.
34. Stadlbauer A, Bernt R, Gruber S, et al. Diffusion-weighted MR imaging with background body signal suppression (DWIBS) for the diagnosis of malignant and benign breast lesions. *Eur Radiol* 2009;**19**:2349–56.
35. Zhu H, Arlinghaus LR, Whisenant JG, et al. Sequence design and evaluation of the reproducibility of water-selective diffusion-weighted imaging of the breast at 3T. *NMR Biomed* 2014;**27**:1030–6.
36. Ouyang Z, Ouyang Y, Zhu M, et al. Diffusion-weighted imaging with fat suppression using short-tau inversion recovery: clinical utility for diagnosis of breast lesions. *Clin Radiol* 2014;**69**:e337–44.
37. Rahbar H, Partridge SC, Eby PR, et al. Characterization of ductal carcinoma *in situ* on diffusion weighted breast MRI. *Eur Radiol* 2011;**21**:2011–9.
38. Vermoolen M, Nievelstein K. Apparent diffusion coefficient measurements in the differentiation between benign and malignant lesions: a systematic review. *Insights Imaging* 2012;**3**:395–409.
39. Woodhams R, Kakita S, Hata H, et al. Diffusion-weighted imaging of mucinous carcinoma of the breast: evaluation of apparent diffusion coefficient and signal intensity in correlation with histologic findings. *AJR Am J Roentgenol* 2009;**193**:260–6.
40. Abdel Razek AA, Gaballa G, Denewer A, et al. Diffusion weighted MR imaging of the breast. *Acad Radiol* 2010;**17**:382–6.